JACS
JOURNAL OF THE AMERICAN CHEMICAL SOCIETY
pubs.acs.org/JACS



Article

# Quantitative and Multiplexing Analysis of MicroRNAs by Direct Full-Length Sequencing in Nanopores

Chenzhi Shi,[§] Donglei Yang,[§] Xiaowei Ma, Yun Chen, Pengfei Hou, Li Pan, Min Li, and Pengfei Wang*

Cite This: J. Am. Chem. Soc. 2025, 147, 15614−15624

Read Online

ACCESS | Metrics & More | Article Recommendations | Supporting Information

**ABSTRACT:** MicroRNAs (miRNAs) play important regulatory roles in biology. Direct sequencing of miRNAs in full-length can reveal comprehensive information on their sequences, abundance, and modifications, which, however, has yet to be achieved due to their extremely short length (~22 nt). Herein, we developed Direct-miR-seq, a nanopore-based direct RNA sequencing (DRS) method that elongates miRNAs at both the 5′ and 3′ ends by ligating with custom nucleic acid adaptors to ensure full-length sequencing of miRNAs with high yield and accuracy. Compared to standard DRS, Direct-miR-seq enabled sequencing of the whole sequence of miRNAs, achieved a 26-fold sequencing yield, and exhibited reduced bias across miRNA species along with low sequencing error rates. We applied Direct-miR-seq to native RNA populations from cells and human serum to demonstrate its capability to selectively capture miRNAs of known sequences in complex RNA environments for revealing quantitative information in abundance and m6A modification at single-molecule and single-base resolution of ~100 miRNA species in a single sequencing event. We envision that Direct-miR-seq may be translated toward a variety of biological and medical applications by sequencing miRNAs and other small RNAs.

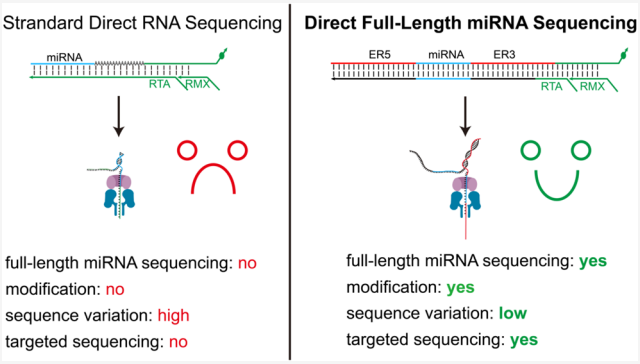


## INTRODUCTION

MicroRNAs (miRNAs) are a class of short (~22 nt), single-stranded, noncoding RNAs that serve as post-transcriptional regulators of gene expression, influencing many critical biological processes, including the occurrence of cancer.[1,2] The biological roles of miRNAs have been found to be highly associated with their sequences, abundance, and epigenetic modifications.[3−5] Hence, revealing such information on miRNAs in a quantitative way could offer important insights into relevant biological processes, which has remained a grand technical challenge. Conventional techniques such as quantitative reverse transcription polymerase chain reaction (qRT-PCR),[6,7] northern blot,[8,9] RNA microarray,[10,11] or specifically designed nucleic acid probes[12−17] can merely acquire limited information on miRNA sequences and abundance with low multiplexing capability, which are also unable to probe modifications. A number of custom nanopore platforms have been developed to detect miRNAs based on ionic current change when molecules pass through the nanopores.[18−23] Since most of them cannot convert ionic current into sequence information, they suffer from low multiplexity and low specificity.[24] Mass spectrometry can quantitatively detect miRNA sequences and modifications, but at a very low throughput. Moreover, it demands a large quantity of miRNAs with high purity that severely limits its applicability for low-abundant biological samples.[25] Next-generation sequencing (NGS) has been widely used for miRNA investigations to quantitatively obtain their sequence and abundance information in high throughput.[26−28] Nevertheless, NGS suffers from high sequencing bias across various miRNA species that derives from inherent bias existing in library construction processes, including ligation of sequencing linkers, reverse transcription, and amplification,[29] which diminishes its quantification accuracy. In addition, NGS is unable to directly probe modifications to miRNAs. It has to couple with antibody-based isolation of methylated miRNAs, which not only requires a large quantity but also exhibits low specificity due to nonspecific capturing of antibodies against methylated RNAs.[30−32]

Nanopore-based direct RNA sequencing (DRS) based on Oxford Nanopore Technology (ONT) has enabled simultaneous detection of RNA sequence, abundance, and modifications with single-molecule and single-base resolution,[33−35] which is independent of amplification, and can offer highly accurate information on RNAs.[36] However, given the existing nanopore configuration possessing high sequencing error at

Received: February 14, 2025
Revised: April 18, 2025
Accepted: April 21, 2025
Published: April 28, 2025





https://doi.org/10.1021/jacs.5c02808
J. Am. Chem. Soc. 2025, 147, 15614−15624

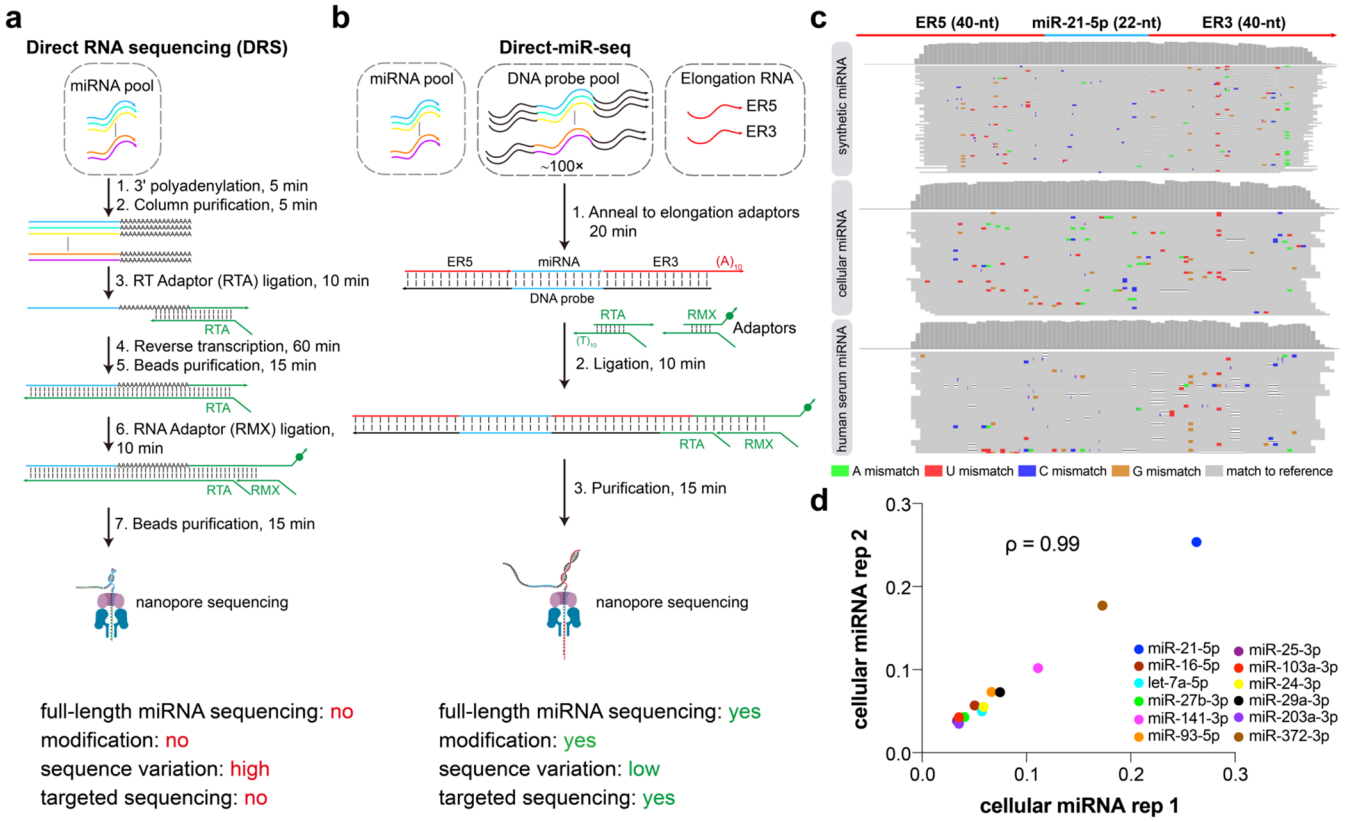


**Figure 1.** Direct-miR-seq for quantitative and multiplexing sequencing of miRNAs in full-length by nanopores. (a) A typical workflow for direct RNA sequencing on the ONT nanopore by using the standard DRS method. (b) Direct-miR-seq enables direct miRNA sequencing in full-length via ligation to custom elongation adaptors at both ends. (c) Integrated genomic viewer (IGV) snapshots of mapped reads from Direct-miR-seq for synthetic, cellular, and human serum miRNAs, with miR-21-5p as the representative miRNA. Error rates for synthetic, cellular, and human serum miR-21-5p from Direct-miR-seq were 3.1, 4.2, and 2.7%, respectively. For the bar charts, positions with mismatch frequencies lower than 0.2 are shown in gray. (d) Scatter plot of cellular miRNA abundance in two biological replicates sequenced by Direct-miR-seq. The correlation strength is indicated by Spearman's correlation coefficient ($\rho$).

both ends of RNAs and loss of sequences at the 5′ end (infeasible for short RNAs),[37−40] direct sequencing of miRNAs in full-length has yet to be achieved (Figure 1a). One pioneering work by Huang and colleagues realized direct miRNA sequencing on a custom nanopore platform by using a nanopore-induced phase-shift sequencing method, where they were able to probe the sequence and modifications of miRNAs with a length of up to 15-nt[41]; thus, it did not enable sequencing of miRNAs in full-length. Furthermore, this method is not compatible with the ONT platform for enabling the accessible, well-established, and high-throughput sequencing of miRNAs. Herein, to enable direct sequencing of miRNAs in full-length on the ONT nanopore platform by using commercially available kits, we developed Direct-miR-seq, where targeted miRNA molecules of known sequences are specifically captured and elongated at both their 5′ and 3′ ends via ligating to custom elongation adaptors that serve as cushioning regions to compensate for the high sequencing errors at both ends of the RNA molecule to ensure full-length miRNA sequencing with high yield, coverage, accuracy, along with m6A modification information (Figure 1b). Direct-miR-seq provides a simple, cost-effective, and high-throughput (~100 miRNA species, which can be further expanded to thousands) sequencing platform to accurately quantify the abundance and modification of miRNAs of interest, which is validated by synthetic, cellular, and human serum miRNAs (Figure 1c,d). We envision that Direct-miR-seq will contribute to the study of the functions of miRNAs in a wide variety of contexts (e.g., cancer) that may be translated into many biological and medical applications.

## RESULTS AND DISCUSSION

**Validation of Direct-miR-seq for miRNA Sequencing in Full-Length.** Several works have demonstrated that nanopore DRS can be used to sequence short RNA molecules such as snoRNA,[42] snRNAs,[42] and tRNAs,[43,44] but it is difficult to capture sequences shorter than ~50 nt, such as miRNAs (~22 nt). The reason is that short sequences produce irregular electric current signals to be wrongly basecalled or discarded, thus making it infeasible to gain confident sequence and modification information (Figure 1a).[38,39] About 15 nucleotides next to the 5′ end cannot be sequenced, and ~4 nucleotides next to the 3′ end exhibited significantly low accuracy. To solve this technical challenge, we proposed to elongate miRNA molecules at their 5′ and 3′ ends by ligating to elongation adaptors, which could compensate for the high sequencing errors at the ends to enable the sandwiched miRNA sequences to be sequenced in full-length, a method we named Direct-miR-seq (Figure 1b). The elongation adaptors consist of three parts, including a DNA probe, a 5′ elongation RNA (ER5), and a 3′ elongation RNA (ER3, containing a poly-A tail for adaptor ligation). The incorporation of DNA probes has several benefits. First, the DNA probe can specifically capture and position miRNA molecules and


https://doi.org/10.1021/jacs.5c02808
J. Am. Chem. Soc. 2025, 147, 15614−15624

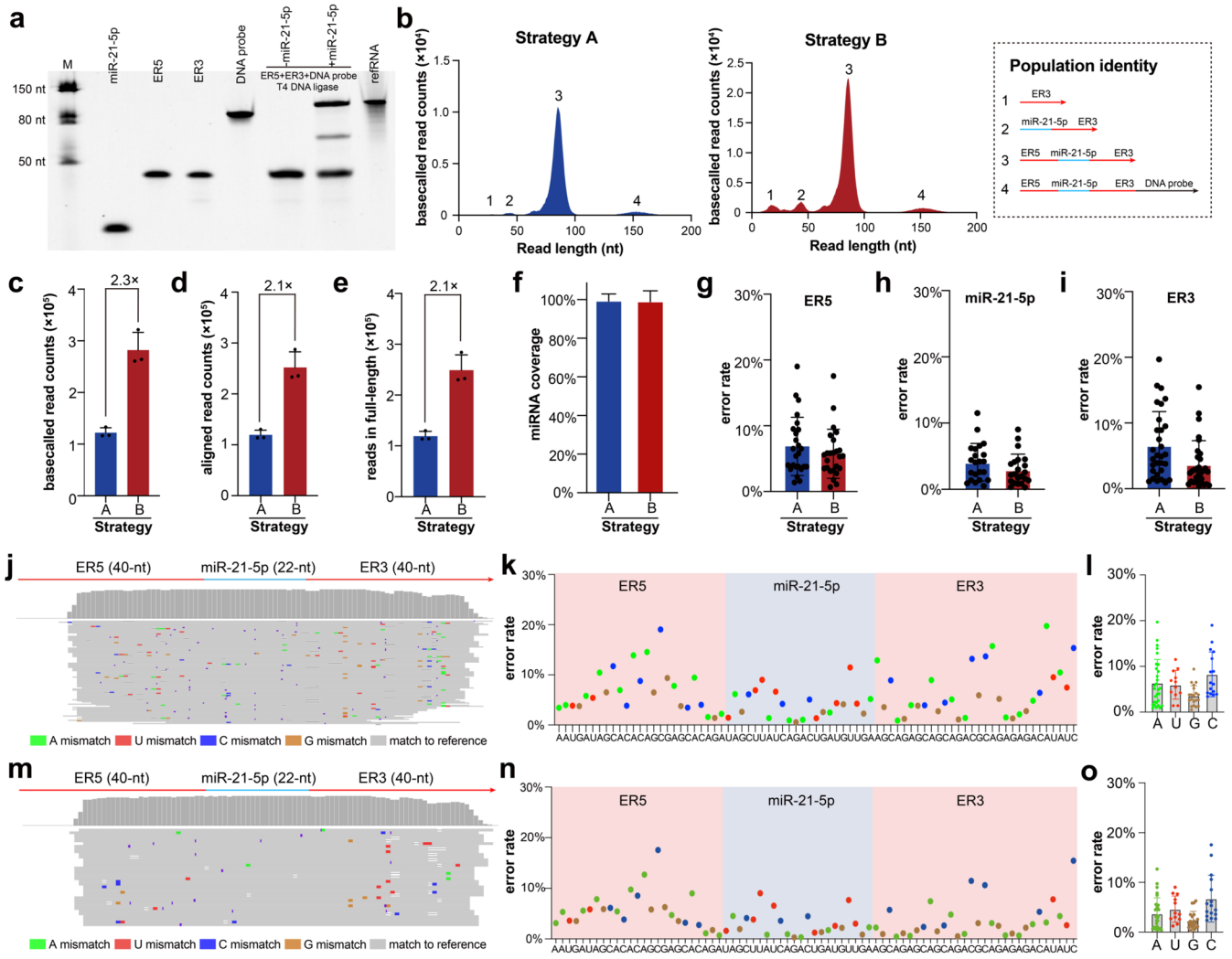


**Figure 2.** Validation of Direct-miR-seq for miRNA sequencing in full-length. (a) Denaturing PAGE to verify ligation of ER5, miR-21−5p, and ER3. To remove the DNA probes, all ligation products were treated with DNase I-XT at room temperature prior to PAGE analysis. Concentrations of miR-21−5p, ER5, ER3, and DNA probe in the ligation reaction were 100, 200, 200, and 200 nM, respectively. (b) Length distribution of basecalled reads from Strategy A and Strategy B. There are four major populations for the basecalled reads, whose identities are illustrated in the dashed line box. Population 3 is the dominant population for both strategies, which corresponds to the correct ligation product. (c−f) Basecalled read counts, mapped read counts, reads-covered miRNA full sequence, and miRNA sequence coverage for miR-21−5p as sequenced via Direct-miR-seq by using Strategy A or Strategy B. (g−i) Sequencing error rates for ER5, miR-21−5p, and ER3, respectively. (j−m) IGV snapshots of mapped reads from strategies A and B. (k−n) Sequencing error rate for each individual nucleotide in miR-21−5p and elongation RNAs from Strategies A and B, respectively. (l−o) Sequencing error rates for A, U, G, and C nucleotides in miR-21−5p and elongation RNAs from Strategy A and Strategy B, respectively. All experimental measurements are presented as mean ± SD with $n = 3$.

elongate RNAs in proximity to promote ligation, given that single-stranded RNAs exhibit low and varied ligation efficiency. Second, the presence of DNA probes can largely minimize self-ligation of miRNAs or elongation RNAs to ensure the correct elongation of miRNAs with high purity. Third, DNA probes can capture targeted miRNAs based on sequence complementarity, which not only alleviates sequence variation-induced bias but also enables targeted sequencing for miRNA species of interest. Taken together, such a design strategy should enable the efficient capture and ligation of targeting miRNAs with high sensitivity, specificity, and low variations among different RNA species. It should be noted that, given that miRNAs are captured by the DNA probes via sequence complementarity, Direct-miR-seq can only be applied to sequence miRNAs of known sequences, and is thus not suitable for universally detecting all miRNA species of known and unknown sequences.

We first validated and optimized Direct-miR-seq by sequencing a synthetic miRNA (miR-21-5p) based on two different strategies (Figure S1). Both strategies employed the same library construction protocol. Strategy A used the default configuration for electric current data processing, while Strategy B was accompanied by a custom pseudosequencing configuration to process the original collected data file prior to basecalling, which supposedly can recapture discarded short reads that were wrongly tagged as "adaptor-only" reads by the default nanopore configuration (Figure S2).[44] Since direct RNA sequencing was suitable for RNA greater than 85 nt[33] and exhibited the highest sequencing error rate for uracil among the four bases,[39] ER5 and ER3 were designed with 40-nt in length, which were composed of low uracil content


https://doi.org/10.1021/jacs.5c02808
J. Am. Chem. Soc. 2025, 147, 15614−15624

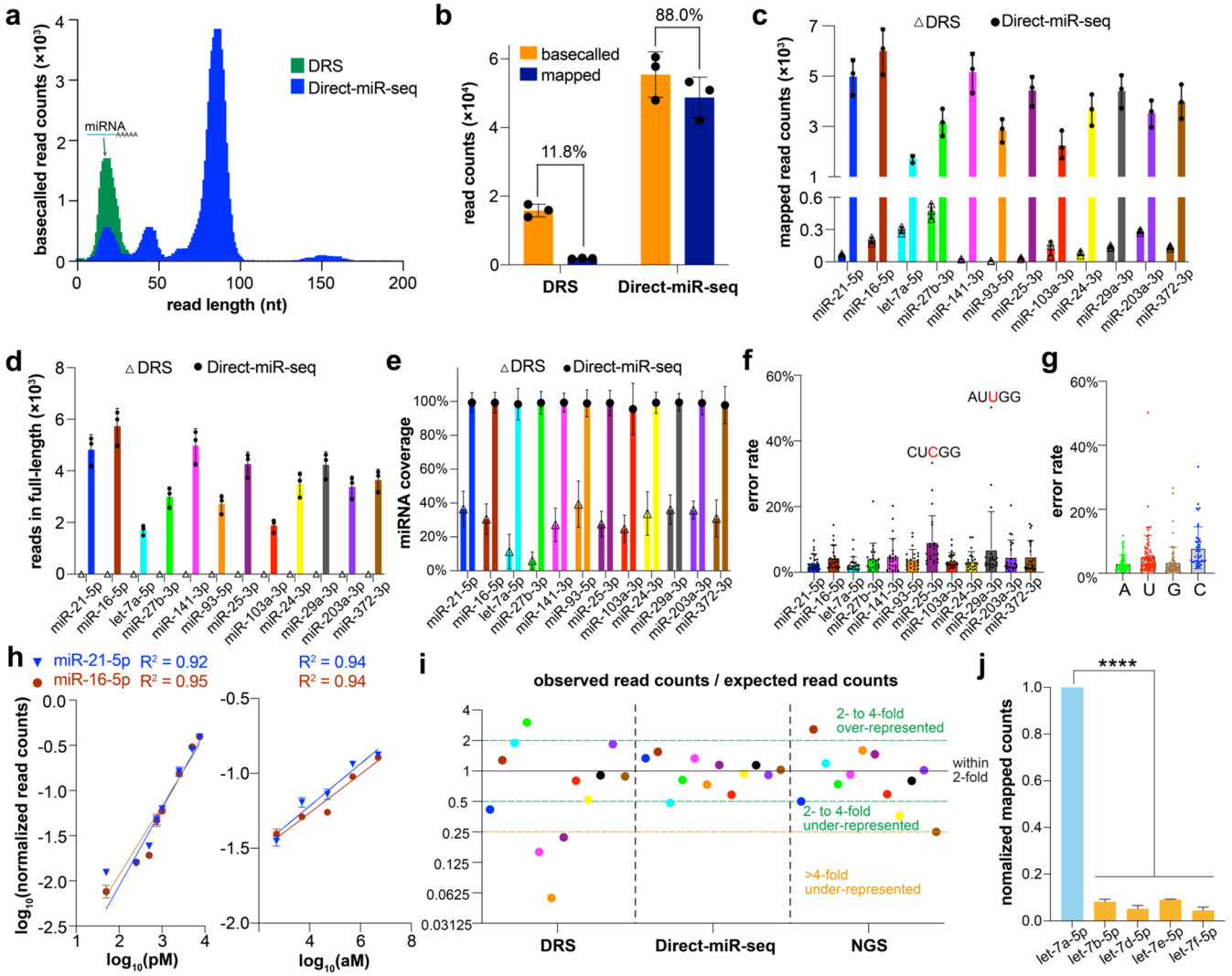


**Figure 3.** Quantitative and multiplexing analysis of miRNAs by using Direct-miR-seq. (a) Length distribution of basecalled reads from DRS and Direct-miR-seq. (b) Basecalled and mapped read counts for a total of 12 synthetic miRNAs. (c) Mapped read counts of individual miRNAs. (d) Mapped read counts that cover the full sequence of miRNAs. (e) Average coverage of nucleotides for individual miRNAs. (f) Sequencing error rate of Direct-miR-seq for synthetic miRNAs computed by taking the mean of all nucleotides. The average error rate for the 12 synthetic miRNAs was 4.7%. Each point represents the error rate for a single nucleotide. The two nucleotides with the highest error rates (red letters) and their surrounding nucleotides (black letters) were annotated. (g) Sequencing error rates of adenines (A), guanines (G), cytosines (C), and uracils (U) contained in the synthetic miRNAs. (h) Validation of the quantitative ability and sensitivity of Direct-miR-seq for sequencing miR-21-5p and miR-16-5p with different input quantities. The read count for each concentration was normalized by setting the value for total counts of each miRNA species in a single sequencing event as 1. (i) Read count variation among 12 miRNAs from DRS, Direct-miR-seq, and NGS was assessed by sequencing miRNAs of the same input quantities. miRNA identities are represented by colored solid circles consistent with (c) through (f). (j) Examination of the specificity of Direct-miR-seq targeting let-7a-5p. Other miRNAs belonging to the let-7 family of single- or double-nucleotide variants of let-7−5p were sequenced with input identical to that of let-7a-5p and compared to let-7a-5p. Mapped counts were normalized by setting the value for let-7a-5p as 1. All experimental measurements are presented as mean ± SD with $n$ = 3.

(7.5%) to minimize uracil-induced sequencing error, to reach a total length of 102-nt for the final ligated RNA product (ER5-miR-ER3). ER3 contained a 10-nt poly-A tail at the 3′ end for sequencing adaptor ligation. Denaturing polyacrylamide gel electrophoresis (PAGE) confirmed the successful and high-yield ligation of elongated RNAs to miRNAs (Figures 2a and S3). miR-21-5p was then subjected to library construction for Direct-miR-seq, which was sequenced on an ONT direct RNA sequencing platform. The length distribution of basecalled reads showed four populations (Figure 2b), with the correct ligation product (population 3: ER5-miR-ER3) being the dominant population for both strategies, indicating high efficiency for miRNA capture and library construction. In addition to the expected ligation product, there were reads with lengths shorter than 48-nt (population 1: ER3; population 2: miR-ER3) or longer than 150-nt (population 4: ER5-miR-ER3-DNA probe; Figure S4). The incomplete ligation products (populations 1 and 2) represented 10.9% of all basecalled reads for Strategy B (Figure S5). For these short reads, given that they only covered ∼8 miRNA nucleotides, they were not considered valid reads for miR-21-5p. Hence, we set 48-nt as the minimum read length for subsequent alignment. Strategy A generated 133,150 basecalled reads (Figure 2c), among which 98% were mapped uniquely to miR-21-5p by using BWA-MEM[45] with short-strand friendly parameters (-x ont2d -k 10 -T 20) (Figure 2d), and 98% of


https://doi.org/10.1021/jacs.5c02808
J. Am. Chem. Soc. 2025, 147, 15614−15624

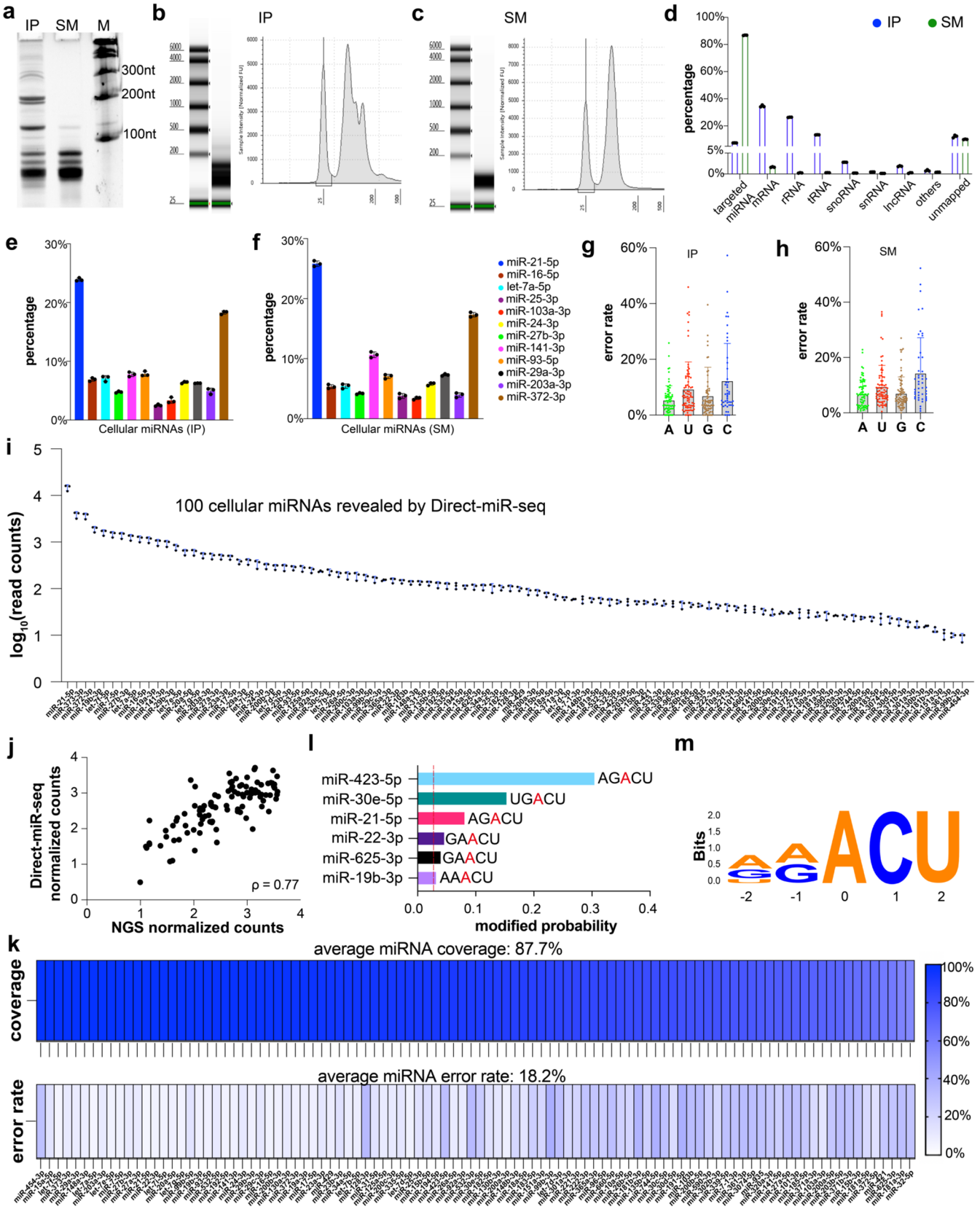


**Figure 4.** Direct-miR-seq for revealing the abundance and modifications of native miRNAs from cells. (a) Denaturing PAGE for small RNAs extracted from the AGS cell line by IP and SM. (b, c) Sample length distribution of (b) IP and (c) SM extractive by Agilent Bioanalyzer. (d) Comparison of Direct-miR-seq data for small RNAs extracted from AGS cells by IP or SM. (e, f) Abundance of 12 target miRNA species from IP (e) and SM (f) extraction. (g, h) Sequencing error rates of adenines (A), guanines (G), cytosines (C), and uracils (U) contained in the 12 miRNA species from IP (g) and SM (h). The average error rates for IP and SM are 7.9 and 9.0%, respectively. (i) Reads of 100 cellular miRNAs revealed by Direct-miR-seq. (j) Scatter plot of normalized miRNA counts from Direct-miR-seq and NGS showing moderate correlation, as characterized by



https://doi.org/10.1021/jacs.5c02808
J. Am. Chem. Soc. 2025, 147, 15614−15624

**Figure** 4. continued

Spearman's correlation coefficient ($\rho$). The read count for each miRNA was normalized by setting the value for total counts of the 100 miRNA species in a single sequencing event as 1, followed by taking a negative logarithm. One point represents one miRNA. (k) Coverage and error rate for each individual cellular miRNA from Direct-miR-seq. (l) 6 cellular miRNAs were identified to be m6A-modified by Direct-miR-seq red dotted line (modified probability = 0.033, recommended by m6Anet) was the threshold to judge whether miRNA was m6A-modified. (m) MEME analysis of the sequence context (from −2 to +2) of all significant m6A sites revealed by Direct-miR-seq. All experimental measurements are presented as mean ± SD with $n$ = 3. $P$ values were calculated by a two-tailed Student's $t$-test.

the mapped reads were able to cover the full sequence of miR-21-5p (Figure 2e). In comparison, Strategy B produced 2.3-fold more basecalled reads, 2.1-fold more mapped reads, and 2.1-fold more reads that covered the full sequence of miR-21-5p. The average coverage of miRNA sequences from mapped reads was 99.8 and 99.4% for Strategy A and Strategy B, respectively (Figure 2f). Furthermore, increased sequencing accuracy in ER5, miRNA, and ER3 was achieved by Direct-miR-seq using Strategy B, with the average error rate for miR-21-5p being as low as 2.96% (Figures 2g−i and S6). We should note that ER5 and ER3 exhibited higher sequencing error rates than miRNA for both strategies, suggesting that ERs functioned well in serving as the cushioning regions to compensate for the elevated sequencing errors at the ends. Detailed analysis on the level of nucleotides is illustrated in Figure 2j−o, which further validates that Direct-miR-seq was able to capture the whole sequence of miRNA with high sequencing accuracy that is comparable to standard DRS on long transcripts.[39,46] The average sequencing accuracy of adenines (A) and guanines (G) was slightly higher than cytosines (C) and uracils (U), consistent with previous studies for direct RNA sequencing (Figure 2l−o).[46] In summary, it has been validated that Direct-miR-seq can enable direct sequencing of miRNAs in full-length with high yield and high accuracy, with Strategy B outperforming Strategy A in all essential categories, and therefore, it was chosen for later sequencing experiments.

**Direct-miR-seq Enables Quantitative and Multiplexing Analysis of miRNAs.** With Direct-miR-seq being comprehensively validated by a single miRNA, we next sought to examine its quantitative and multiplexing capabilities in sequencing a group of 12 different synthetic miRNAs simultaneously, which were equally mixed for library construction and sequencing. Standard DRS and next-generation sequencing (NGS) were used for comparison (Table S1). As revealed from the length distribution of basecalled reads, one can tell that the majority reads from Direct-miR-seq covered the whole sequence of miRNAs (Figure 3a). In contrast, reads from the DRS can only partially cover miRNA sequences. Furthermore, Direct-miR-seq achieved a significantly higher sequencing yield than DRS, with 3.5-fold more basecalled reads and 26-fold more mapped reads, along with a much-improved mapping ratio of 88.0% (Figure 3b,c). The poor mappability of DRS reads is attributed to the sequence loss on the 5′ end due to the inability to cover the full sequence of miRNAs. The majority (Avg: ∼89%, Figure S7) of the mapped reads from Direct-miR-seq were able to cover the full sequence of 12 miRNAs (Figure 3d), exhibiting an average coverage of miRNA sequences of 99% (Figures 3e and S8). In contrast, reads from DRS only exhibited an average coverage of miRNA sequences of ∼28%, with only one read being successfully mapped to miRNAs in full-length (Figure 3d). Moreover, Direct-miR-seq demonstrated high sequencing accuracy for these 12 miRNAs (average 4.7%), with the error rate of let-7a-5p being as low as 2.49% (Figure 3f,g). In contrast, DRS exhibited significantly lower sequencing accuracy, with an average error rate of 69.8% for these synthetic miRNAs (Figure S9), which further justified the necessity of using elongation adaptors for short miRNAs. Note that variations existed between different miRNA species, with miR-25-3p and let-7a-5p having the highest and lowest sequencing errors, respectively, which can be attributed to the inherent sequencing bias of nanopores against different nucleotides and sequences. For instance, the two nucleotides with the observed highest error rate should be attributed to low sequencing accuracy for uracils and bases next to uracils, consistent with the accuracy consensus of nanopore sequencing.[39]

To assess its accuracy and sensitivity in quantifying miRNAs, we examined the performance of Direct-miR-seq in sequencing synthetic miR-21-5p and miR-16-5p with a series of different concentrations from 500 aM to 7.5 nM as distinguished by a 15-nt barcode on ER3 (Table S2). Given its single-molecule detection nature, in principle, nanopore sequencing will be able to detect miRNAs of extremely low abundance if there are miRNA molecules in the pool. It was revealed that Direct-miR-seq provided expected estimates of miRNA abundance that agreed well with the input quantities (Figure 3h), showing potent capability in accurately quantifying miRNAs. Furthermore, Direct-miR-seq achieved high miRNA coverage (Avg: 99%) and low error rate (Avg: 3.4%) in sequencing miRNAs at various concentrations, verifying the robustness of Direct-miR-seq (Figure S10). Therefore, Direct-miR-seq exhibited high detection sensitivity and sequencing accuracy due to its single-molecule detection nature that is readily applicable to biological miRNAs of reported abundance, typically in the fM−pM range.

We further analyzed read counts for the 12 synthetic miRNAs with the same input quantity to evaluate quantification bias across different miRNAs by Direct-miR-seq, DRS, and NGS. The read ratio for each miRNA was calculated by dividing the expected read counts (total counts divided by 12) by the observed read counts (Figure 3i). As illustrated, for Direct-miR-seq, 11 out of 12 miRNAs fell within 2-fold of the expected abundance, with only let-7a-5p exhibiting slightly lower counts than expected. In comparison, DRS and illumina-based small-RNA sequencing (NGS) showed higher variations among miRNA species, with DRS having the highest bias for quantification (Figure S11). The potent quantification accuracy of Direct-miR-seq can be attributed to the incorporation of DNA probes and elongation RNAs for minimizing polyadenylation and ligation bias-induced sequencing variations that exist in DRS and NGS methods. To evaluate the detection specificity of Direct-miR-seq, we examined the let-7a probe for discriminating let-7a-5p from other family members with single- or double-nucleotide variations, including let-7b, let-7d, let-7e, and let-7f. As shown in Figure 3j, a great majority of reads (>80%) were mapped to let-7a,


https://doi.org/10.1021/jacs.5c02808
J. Am. Chem. Soc. 2025, 147, 15614−15624

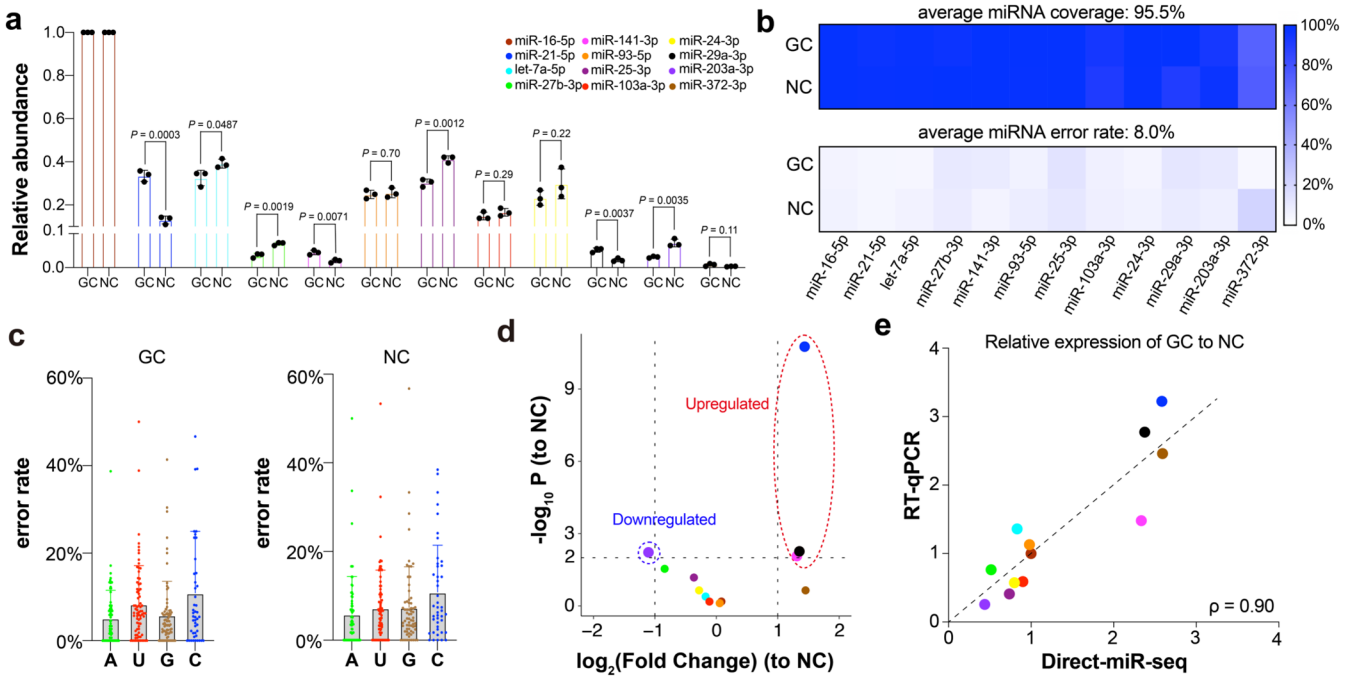


**Figure 5.** Detection of serum-derived miRNAs by Direct-miR-seq. (a) Relative abundance of 12 targeted miRNAs in serum from gastric cancer (GC) and noncancer controls (NC), as revealed by Direct-miR-seq. Relative abundance was calculated by dividing the counts of miRNAs by the counts of miR-16-5p, with miR-16-5p serving as the housekeeping gene for expression normalization. (b) Sequencing coverage and error rate of 12 miRNAs in GC and NC samples. (c) Sequencing error rates of adenines (A), guanines (G), cytosines (C), and uracils (U) contained in the 12 miRNA species from GC and HD. (d) Differentially expressed miRNAs of GC relative to NC. Differentially expressed miRNAs were defined as having an adjusted *P* value less than 0.01 and an absolute fold change greater than 2. (e) Relative expression profiles of GC to NC for the targeted miRNAs between Direct-miR-seq and RT-qPCR. All experimental measurements are presented as mean ± SD with $n = 3$. *P* values were calculated by a two-tailed Student's *t*-test.

and no reads were mapped to miRNAs outside the let-7 family, indicating Direct-miR-seq's high specificity in detecting targeting miRNAs.

In summary, we have demonstrated that Direct-miR-seq was able to sequence different miRNA species simultaneously in a highly quantitative, accurate, and specific manner.

**Direct-miR-seq Reveals Abundance and Modifications of Native Cellular miRNAs.** We next sought to apply Direct-miR-seq to detecting native miRNAs. Isopropanol precipitation (IP) and silicon membrane (SM) are two widely used RNA extraction protocols for biological samples, both of which have been evaluated for sequencing miRNAs from a gastric cancer cell line (AGS cells). In comparison, RNAs extracted by SM exhibited better enrichment of short RNAs (<100 nt) than IP (Figure 4a−c), suggesting that it should produce a higher sequencing output of miRNAs. Indeed, by using SM-extracted RNAs for Direct-miR-seq of 12 probes, there were 86.78% reads mapped to miRNAs, while in contrast, only 7.48% reads were mapped to miRNAs if using the IP method, with its majority reads corresponding to other RNAs such as mRNAs, rRNAs, tRNAs, etc. (Figure 4d). Though these RNAs are not specifically captured by Direct-miR-seq, a large portion of them may still be ligated to the sequencing adaptors or may pass through the nanopore by themselves; both will impede the sequencing of miRNAs. Hence, enrichment of miRNAs in the starting pool prior to library construction is critical to Direct-miR-seq for acquiring high sequencing yields. For mapped miRNA reads, the SM and IP methods exhibited similar relative miRNA abundances after Direct-miR-seq sequencing (Figure 4e,f). The overall sequencing error rate of 12 cellular miRNAs (7.9% for IP, 9.0% for SM) was slightly higher than that of their synthetic counterparts (Figures 4g,h andS12−S13).

The detection capability of Direct-miR-seq was expanded by sequencing 100 different cellular miRNAs from AGS cells (Tables S2 and S3), whose read counts are plotted in Figure 4i. miR-21-5p and miR-454-3p exhibited the highest and lowest abundances, respectively. Direct-miR-seq showed high specificity with negligible untargeted miRNAs (0.011% out of all mapped reads) captured by the DNA probes (Figure S14). There was a strong correlation between reads from Direct-miR-seq and NGS ($\rho = 0.77$, Figure 4j). An average sequence coverage of 87.8% was achieved for 100 cellular miRNAs, along with an average sequencing error rate of 18.2% (Figures 4k and S15). The sequencing error rate of cellular miRNAs is higher than that of synthetic miRNAs, which is probably because native miRNAs potentially exhibit various modifications (e.g., $m^6A$, $m^1A$, and $m^3C$) that may impair sequencing accuracy.[47−49] In addition to revealing miRNA abundance, Direct-miR-seq can capture m6A information at consensus DRACH motifs at single-molecule and single-base resolutions by using a neutral network model m6Anet based on supervised machine learning with high accuracy and high precision.[50,51] Among 100 cellular miRNAs, Direct-miR-seq identified 6 miRNAs with m6A modification at single-molecule and single-base levels, given that their modified probability provided by m6Anet is higher than the threshold ($P > 0.033$) (Figure 4l,m).

**Quantitative Detection of Serum-Derived miRNAs by Direct-miR-seq.** To further demonstrate its applicability, Direct-miR-seq was used to sequence native miRNAs extracted from the serum of two clinical groups, gastric cancer (GC) and noncancer controls (NC), with each group containing 16


https://doi.org/10.1021/jacs.5c02808
J. Am. Chem. Soc. 2025, 147, 15614−15624

donors. Individual serum samples within the same group were mixed prior to RNA extraction to ensure that a single sequencing run could collect miRNA information representing the whole clinical group (Table S4). A total of 12 serum miRNAs were sequenced by Direct-miR-seq, with miR-16-5p serving as the biological reference since it has been widely reported to exhibit stable expression in humans.[52] As revealed, the relative abundance of miRNAs derived from Direct-miR-seq showed highly differential profiles for GC and NC groups (Figure 5a). High coverage and low error rate of miRNAs for both GC and NC were achieved by Direct-miR-seq, as illustrated in Figures 5b,c and S16 and S17. Based on a negative binomial model of miRNA counts, we identified three miRNAs that showed significantly elevated expression, and one miRNA that exhibited significantly reduced expression in GC (Figure 5d). To verify the quantitative ability of Direct-miR-seq in native miRNAs, we compared the relative expression of each miRNA in GC relative to NC with RT-qPCR (Figure S18) using miR-16-5p as the biological reference. Relative miRNA expression profiles of GC versus NC derived from the two assays showed good agreement ($\rho$ = 0.90, Figure 5e). Note that heterogeneous relative abundance profiles of different miRNA species were observed by Direct-miR-seq and RT-qPCR, which may be attributed to the nonoptimal design of primers causing biased amplifications of different miRNAs. m6A modification information on serum miRNAs has not been derived from Direct-miR-seq, presumably due to the low sequencing depth.[50,51]

## CONCLUSIONS

In the past few years, various methods have been developed for the direct sequencing of RNAs to reveal their sequence and modification information (e.g., Nano-tRNAseq, NERD-seq) based on ONT nanopores, but none of them are applicable to miRNAs due to their extremely short length. When short RNA passes through the nanopores, it generates an irregular electric current that cannot be accurately basecalled, especially for nucleotides close to the ends. In Direct-miR-seq, miRNA molecules are elongated at both the 5′ and 3′ ends by ligating with custom adaptors to compensate for the high sequencing errors at RNA ends. Being sandwiched and sealed in the middle, miRNAs can then be sequenced in full-length with high yield and accuracy. Direct-miR-seq has been validated on synthetic, cellular, and serum miRNAs to quantitatively reveal their sequence, abundance, and modification information with high accuracy and replicability. For synthetic miRNAs, in comparison to standard DRS, Direct-miR-seq achieved a 26-fold sequencing yield and a 7.5-fold mapping ratio, along with higher miRNA coverage and lower sequencing error rate. Furthermore, Direct-miR-seq exhibited potent capability in miRNA quantification, showing much lower bias against different miRNA species, compared to DRS and NGS methods (Table S5). For native miRNAs extracted from cells and human serum, Direct-miR-seq enabled high-throughput (~100 miRNA species) sequencing of extracted small-RNA populations to reveal their abundance and modification information. For instance, we identified 6 miRNA species with m6A modification at the single-molecule level, confirming that Direct-miR-seq can obtain epigenetic information with single-base resolution. With the development of new sequencing flow cells and basecalling algorithms, chemical modifications beyond m6A may be detected by Direct-miR-seq in the near future. The number of targeting miRNAs could be readily expanded to thousands by using a larger number of DNA probes for sequencing library construction. To the best of our knowledge, Direct-miR-seq is the first reported nanopore method that enables direct sequencing of the whole sequence of miRNAs. Direct-miR-seq is a highly programmable and applicable nanopore method for direct full-length miRNA sequencing. This method is not limited to the MinION platform used here, which can be easily adapted by other ONT platforms, such as Flongle, GridION, and PromethION, or any other non-ONT nanopore platform capable of RNA sequencing, either commercial or customized. With the development of new sequencing nanopores and basecalling algorithms, the sequencing yield and accuracy of direct miRNA sequencing may be further improved in the near future. We envision that Direct-miR-seq will shed light on miRNA detection that may be used for many biological and medical applications, such as diagnostics and prognostics of cancers.

We note that miRNAs detected by Direct-miR-seq all have known sequences. Although the use of DNA probes can enhance miRNA capture and ligation efficiency and reduce variations between different miRNA species, it limits the multiplexing capability of Direct-miR-seq and renders it unable to discover new miRNAs. A new version of Direct-miR-seq is currently under development to universally capture the total population of small RNA, containing both known and unknown sequences (Figure S19). In addition, Direct-miR-seq can only capture miRNAs with terminal modifications of 5′-P and 3′-OH, which may leave a small portion of miRNAs with noncanonical end modifications (e.g., 5′-OH, 3′-P, 2′,3′-cP) not being quantified.[48] To overcome this challenge, in the future, miRNAs may be pretreated with enzymes, such as T4 polymerase kinase, to restore noncanonical terminal modifications to 5′-P and 3′-OH before library preparation. It should also be noted that Direct-miR-seq is not able to improve the overall RNA sequencing accuracy of nanopore technology, which is determined by intrinsic nanopore configurations and basecalling algorithms. Direct-miR-seq achieved higher miRNA sequencing accuracy by employing an innovative library construction strategy, which is to sandwich miRNAs with elongation RNAs. In other words, the sequencing accuracy of elongation RNAs was sacrificed to help improve the sequencing accuracy of miRNAs sealed in the middle.

## ASSOCIATED CONTENT

### Data Availability Statement

The data that support the plots and other findings of this study are either included in the Supporting Information or are available from the corresponding author upon reasonable request.

### Supporting Information

The Supporting Information is available free of charge at https://pubs.acs.org/doi/10.1021/jacs.5c02808.

Additional experimental details; materials; methods; sequencing library construction, data processing; additional sequencing data; DNA strands sequences; and patient information (PDF)



https://doi.org/10.1021/jacs.5c02808
J. Am. Chem. Soc. 2025, 147, 15614−15624

## AUTHOR INFORMATION


### Corresponding Author

**Pengfei Wang** − *Department of Laboratory Medicine, Renji Hospital, School of Medicine, Shanghai Jiao Tong University, Shanghai 200127, China; Institute of Molecular Medicine, Shanghai Key Laboratory for Nucleic Acid Chemistry and Nanomedicine, Renji Hospital, School of Medicine, Shanghai Jiao Tong University, Shanghai 200127, China;* orcid.org/0000-0002-3125-763X; Email: pengfei.wang@sjtu.edu.cn

### Authors

**Chenzhi Shi** − *Department of Laboratory Medicine, Renji Hospital, School of Medicine, Shanghai Jiao Tong University, Shanghai 200127, China; Institute of Molecular Medicine, Shanghai Key Laboratory for Nucleic Acid Chemistry and Nanomedicine, Renji Hospital, School of Medicine, Shanghai Jiao Tong University, Shanghai 200127, China;* orcid.org/0009-0001-6133-5993

**Donglei Yang** − *Institute of Molecular Medicine, Shanghai Key Laboratory for Nucleic Acid Chemistry and Nanomedicine, Renji Hospital, School of Medicine, Shanghai Jiao Tong University, Shanghai 200127, China*

**Xiaowei Ma** − *Department of Laboratory Medicine, Renji Hospital, School of Medicine, Shanghai Jiao Tong University, Shanghai 200127, China*

**Yun Chen** − *Institute of Molecular Medicine, Shanghai Key Laboratory for Nucleic Acid Chemistry and Nanomedicine, Renji Hospital, School of Medicine, Shanghai Jiao Tong University, Shanghai 200127, China*

**Pengfei Hou** − *Institute of Molecular Medicine, Shanghai Key Laboratory for Nucleic Acid Chemistry and Nanomedicine, Renji Hospital, School of Medicine, Shanghai Jiao Tong University, Shanghai 200127, China*

**Li Pan** − *Institute of Molecular Medicine, Shanghai Key Laboratory for Nucleic Acid Chemistry and Nanomedicine, Renji Hospital, School of Medicine, Shanghai Jiao Tong University, Shanghai 200127, China*

**Min Li** − *Department of Laboratory Medicine, Renji Hospital, School of Medicine, Shanghai Jiao Tong University, Shanghai 200127, China*

Complete contact information is available at: https://pubs.acs.org/10.1021/jacs.5c02808

### Author Contributions

[§]C.S. and D.Y. contributed equally to this work.


### Notes

The detailed materials, methods, and supporting figures are included in the Supporting Information. The study was approved by the Ethics Committee of Renji Hospital (KY2023-003-B), School of Medicine, Shanghai Jiao Tong University. The codes used in this study are available upon request.

The authors declare no competing financial interest.

## ACKNOWLEDGMENTS

The authors thank the support from the National Key Research and Development Program of China (2021YFA0910100), the National Natural Science Foundation of China (22304112), and the Innovative Research Team of High-Level Local Universities in Shanghai (SHSMU-ZLCX20212602).

## REFERENCES


(1) Treiber, T.; Treiber, N.; Meister, G. Regulation of microRNA Biogenesis and Its Crosstalk with Other Cellular Pathways. *Nat. Rev. Mol. Cell Biol.* **2019**, *20* (1), 5−20.

(2) Lee, Y.-Y.; Kim, H.; Kim, V. N. Sequence Determinant of Small RNA Production by DICER. *Nature* **2023**, *615* (7951), 323−330.

(3) Han, X.; Guo, J.; Fan, Z. Interactions between m6A Modification and miRNAs in Malignant Tumors. *Cell Death Dis.* **2021**, *12* (6), No. 598.

(4) Deng, X.; Qing, Y.; Horne, D.; Huang, H.; Chen, J. The Roles and Implications of RNA m6A Modification in Cancer. *Nat. Rev. Clin. Oncol.* **2023**, *20* (8), 507−526.

(5) Gebert, L. F. R.; MacRae, I. J. Regulation of microRNA Function in Animals. *Nat. Rev. Mol. Cell Biol.* **2019**, *20* (1), 21−37.

(6) Jet, T.; Gines, G.; Rondelez, Y.; Taly, V. Advances in Multiplexed Techniques for the Detection and Quantification of microRNAs. *Chem. Soc. Rev.* **2021**, *50* (6), 4141−4161.

(7) Shen, W.; Hou, Y.; Yi, Y.; Li, F.; He, C.; Wang, J. G-Clamp Heterocycle Modification Containing Interstrand Photo-Cross-Linker to Capture Intracellular MicroRNA Targets. *J. Am. Chem. Soc.* **2024**, *146* (18), 12778−12789.

(8) Ahmad, W.; Gull, B.; Baby, J.; Mustafa, F. A Comprehensive Analysis of Northern versus Liquid Hybridization Assays for mRNAs, Small RNAs, and miRNAs Using a Non-Radiolabeled Approach. *Curr. Issues Mol. Biol.* **2021**, *43* (2), 457−484.

(9) Lee, E. J.; Baek, M.; Gusev, Y.; Brackett, D. J.; Nuovo, G. J.; Schmittgen, T. D. Systematic Evaluation of microRNA Processing Patterns in Tissues, Cell Lines, and Tumors. *RNA* **2008**, *14* (1), 35−42.

(10) Xu, W.; Yin, P.; Dai, M. Super-resolution Geometric Barcoding for Multiplexed miRNA Profiling. *Angew. Chem., Int. Ed.* **2018**, *57* (43), 14075−14079.

(11) Lee, J. M.; Jung, Y. Two-Temperature Hybridization for Microarray Detection of Label-Free MicroRNAs with Attomole Detection and Superior Specificity. *Angew. Chem., Int. Ed.* **2011**, *50* (52), 12487−12490.

(12) Koch, C.; Reilly-O'Donnell, B.; Gutierrez, R.; Lucarelli, C.; Ng, F. S.; Gorelik, J.; Ivanov, A. P.; Edel, J. B. Nanopore Sequencing of DNA-Barcoded Probes for Highly Multiplexed Detection of microRNA, Proteins and Small Biomarkers. *Nat. Nanotechnol.* **2023**, *18* (12), 1483−1491.

(13) Shi, C.; Yang, D.; Ma, X.; Pan, L.; Shao, Y.; Arya, G.; Ke, Y.; Zhang, C.; Wang, F.; Zuo, X.; Li, M.; Wang, P. A Programmable DNAzyme for the Sensitive Detection of Nucleic Acids. *Angew. Chem., Int. Ed.* **2024**, *63* (12), No. e202320179.

(14) Ma, X.; Zhou, F.; Yang, D.; Chen, Y.; Li, M.; Wang, P. miRNA Detection for Prostate Cancer Diagnosis by miRoll-Cas: miRNA Rolling Circle Transcription for CRISPR-Cas Assay. *Anal. Chem.* **2023**, *95* (35), 13220−13226.

(15) Cai, S.; Pataillot-Meakin, T.; Shibakawa, A.; Ren, R.; Bevan, C. L.; Ladame, S.; Ivanov, A. P.; Edel, J. B. Single-Molecule Amplification-Free Multiplexed Detection of Circulating microRNA Cancer Biomarkers from Serum. *Nat. Commun.* **2021**, *12* (1), No. 3515.

(16) Zeng, Y.; Yue, H.; Cao, B.; Li, Y.; Yang, M.; Mao, C. Target-Triggered Formation of Artificial Enzymes on Filamentous Phage for Ultrasensitive Direct Detection of Circulating miRNA Biomarkers in Clinical Samples. *Angew. Chem., Int. Ed.* **2022**, *61* (45), No. e202210121.

(17) Liu, Y.; Li, B.; Wang, Y.-J.; Fan, Z.; Du, Y.; Li, B.; Liu, Y.-J.; Liu, B. In-Situ Single-Molecule Imaging of microRNAs in Switchable Migrating Cells under Biomimetic Confinement. *Anal. Chem.* **2022**, *94* (9), 4030−4038.

(18) Yan, S.; Wang, L.; Wang, Y.; Cao, Z.; Zhang, S.; Du, X.; Fan, P.; Zhang, P.; Chen, H.-Y.; Huang, S. Non-binary Encoded Nucleic Acid Barcodes Directly Readable by a Nanopore. *Angew. Chem., Int. Ed.* **2022**, *61* (20), No. e202116482.

(19) Takeuchi, N.; Hiratani, M.; Kawano, R. Pattern Recognition of microRNA Expression in Body Fluids Using Nanopore Decoding at Subfemtomolar Concentrations. *JACS Au* **2022**, *2* (8), 1829−1838.
(20) Zhang, X.; Wang, Y.; Fricke, B. L.; Gu, L.-Q. Programming Nanopore Ion Flow for Encoded Multiplex MicroRNA Detection. *ACS Nano* **2014**, *8* (4), 3444−3450.
(21) Wang, Y.; Zheng, D.; Tan, Q.; et al. Nanopore-Based Detection of Circulating microRNAs in Lung Cancer Patients. *Nat. Nanotechnol.* **2011**, *6* (10), 668−674.
(22) Liu, Y.; Wang, X.; Campolo, G.; Teng, X.; Ying, L.; Edel, J. B.; Ivanov, A. P. Single-Molecule Detection of α-Synuclein Oligomers in Parkinson's Disease Patients Using Nanopores. *ACS Nano* **2023**, *17* (22), 22999−23009.
(23) Ying, Y.-L.; Hu, Z.-L.; Zhang, S.; Qing, Y.; Fragasso, A.; Maglia, G.; Meller, A.; Bayley, H.; Dekker, C.; Long, Y.-T. Nanopore-Based Technologies beyond DNA Sequencing. *Nat. Nanotechnol.* **2022**, *17* (11), 1136−1146.
(24) Takiguchi, S.; Takeuchi, N.; Shenshin, V.; Gines, G.; Genot, A. J.; Nivala, J.; Rondelez, Y.; Kawano, R. Harnessing DNA Computing and Nanopore Decoding for Practical Applications: From Informatics to microRNA-Targeting Diagnostics. *Chem. Soc. Rev.* **2025**, *54* (1), 8−32.
(25) Yuan, X.; Su, Y.; Johnson, B.; Kirchner, M.; Zhang, X.; Xu, S.; Jiang, S.; Wu, J.; Shi, S.; Russo, J. J.; Chen, Q.; Zhang, S. Mass Spectrometry-Based Direct Sequencing of tRNAs De Novo and Quantitative Mapping of Multiple RNA Modifications. *J. Am. Chem. Soc.* **2024**, *146* (37), 25600−25613.
(26) Park, C.; Chung, S.; Kim, H.; Kim, N.; Son, H. Y.; Kim, R.; Lee, S.; Park, G.; Rho, H. W.; Park, M.; Han, J.; Song, Y.; Lee, J.; Jun, S.-H.; Huh, Y.-M.; Jeong, H. H.; Lim, E.-K.; Kim, E.; Haam, S. All-in-One Fusogenic Nanoreactor for the Rapid Detection of Exosomal MicroRNAs for Breast Cancer Diagnosis. *ACS Nano* **2024**, *18* (38), 26297−26314.
(27) Reggiardo, R. E.; Maroli, S. V.; Peddu, V.; Davidson, A. E.; Hill, A.; LaMontagne, E.; Aaraj, Y. A.; Jain, M.; Chan, S. Y.; Kim, D. H. Profiling of Repetitive RNA Sequences in the Blood Plasma of Patients with Cancer. *Nat. Biomed. Eng.* **2023**, *7* (12), 1627−1635.
(28) Sun, J.; Teng, M.; Zhu, W.; Zhao, X.; Zhao, L.; Li, Y.; Zhang, Z.; Liu, Y.; Bi, S.; Wu, F. MicroRNA and Gut Microbiota Alter Intergenerational Effects of Paternal Exposure to Polyethylene Nanoplastics. *ACS Nano* **2024**, *18* (27), 18085−18100.
(29) Hu, J. F.; Yim, D.; Ma, D.; Huber, S. M.; Davis, N.; Bacusmo, J. M.; Vermeulen, S.; Zhou, J.; Begley, T. J.; DeMott, M. S.; Levine, S. S.; De Crécy-Lagard, V.; Dedon, P. C.; Cao, B. Quantitative Mapping of the Cellular Small RNA Landscape with AQRNA-Seq. *Nat. Biotechnol.* **2021**, *39* (8), 978−988.
(30) Tan, L.; Guo, Z.; Shao, Y.; Ye, L.; Wang, M.; Deng, X.; Chen, S.; Li, R. Analysis of Bacterial Transcriptome and Epitranscriptome Using Nanopore Direct RNA Sequencing. *Nucleic Acids Res.* **2024**, *52* (15), 8746−8762.
(31) Zhang, Z.; Chen, L. Q.; Zhao, Y.; Zhao, Y. L.; Yang, C.; Yang, C. G.; Roundtree, I. A.; Roundtree, I. A.; Zhang, Z.; Zhang, Z.; Ren, J.; Ren, J.; Xie, W.; Xie, W.; He, C.; He, C.; Luo, G. Single-Base Mapping of m6A by an Antibody-Independent Method. *Sci. Adv.* **2019**, *5* (7), No. eaax0250.
(32) Begik, O.; Lucas, M. C.; Liu, H.; Ramirez, J. M.; Mattick, J. S.; Novoa, E. M. Integrative Analyses of the RNA Modification Machinery Reveal Tissue- and Cancer-Specific Signatures. *Genome Biol.* **2020**, *21* (1), No. 97.
(33) Jain, M.; Abu-Shumays, R.; Olsen, H. E.; Akeson, M. Advances in Nanopore Direct RNA Sequencing. *Nat. Methods* **2022**, *19* (10), 1160−1164.
(34) Garalde, D. R.; Snell, E. A.; Jachimowicz, D.; Sipos, B.; Lloyd, J. H.; Bruce, M.; Pantic, N.; Admassu, T.; James, P.; Warland, A.; Jordan, M.; Ciccone, J.; Serra, S.; Keenan, J.; Martin, S.; McNeill, L.; Wallace, E. J.; Jayasinghe, L.; Wright, C.; Blasco, J.; Young, S.; Brocklebank, D.; Juul, S.; Clarke, J.; Heron, A. J.; Turner, D. J. Highly Parallel Direct RNA Sequencing on an Array of Nanopores. *Nat. Methods* **2018**, *15* (3), 201−206.
(35) Schönegger, E. S.; Crisp, A.; Müller, M.; Fertl, J.; Serdjukow, S.; Croce, S.; Kollaschinski, M.; Carell, T.; Frischmuth, T. Click Chemistry Enables Rapid Amplification of Full-Length Reverse Transcripts for Long-Read Third Generation Sequencing. *Bioconjugate Chem.* **2022**, *33* (10), 1789−1795.
(36) Baek, A.; Lee, G.-E.; Golconda, S.; Rayhan, A.; Manganaris, A. A.; Chen, S.; Tirumuru, N.; Yu, H.; Kim, S.; Kimmel, C.; Zablocki, O.; Sullivan, M. B.; Addepalli, B.; Wu, L.; Kim, S. Single-Molecule Epitranscriptomic Analysis of Full-Length HIV-1 RNAs Reveals Functional Roles of Site-Specific m6As. *Nat. Microbiol.* **2024**, *9* (5), 1340−1355.
(37) Grünberger, F.; Ferreira-Cerca, S.; Grohmann, D. Nanopore Sequencing of RNA and cDNA Molecules in *Escherichia Coli*. *RNA* **2022**, *28* (3), 400−417.
(38) Jiang, F.; Zhang, J.; Liu, Q.; Liu, X.; Wang, H.; He, J.; Kang, L. Long-Read Direct RNA Sequencing by 5′-Cap Capturing Reveals the Impact of Piwi on the Widespread Exonization of Transposable Elements in Locusts. *RNA Biol.* **2019**, *16* (7), 950−959.
(39) Liu-Wei, W.; van der Toorn, W.; Bohn, P.; Hölzer, M.; Smyth, R. P.; Von Kleist, M. Sequencing Accuracy and Systematic Errors of Nanopore Direct RNA Sequencing. *BMC Genomics* **2024**, *25* (1), No. 528.
(40) Thomas, N. K.; Poodari, V. C.; Jain, M.; Olsen, H. E.; Akeson, M.; Abu-Shumays, R. L. Direct Nanopore Sequencing of Individual Full Length tRNA Strands. *ACS Nano* **2021**, *15* (10), 16642−16653.
(41) Zhang, J.; Yan, S.; Chang, L.; Guo, W.; Wang, Y.; Wang, Y.; Zhang, P.; Chen, H.-Y.; Huang, S. Direct microRNA Sequencing Using Nanopore-Induced Phase-Shift Sequencing. *iScience* **2020**, *23* (3), No. 100916.
(42) Saville, L.; Wu, L.; Habtewold, J.; Cheng, Y.; Gollen, B.; Mitchell, L.; Stuart-Edwards, M.; Haight, T.; Mohajerani, M.; Zovoilis, A. NERD-Seq: A Novel Approach of Nanopore Direct RNA Sequencing That Expands Representation of Non-Coding RNAs. *Genome Biol.* **2024**, *25* (1), No. 233.
(43) Sun, Y.; Piechotta, M.; Naarmann-de Vries, I.; Dieterich, C.; Ehrenhofer-Murray, A. E. Detection of Queuosine and Queuosine Precursors in tRNAs by Direct RNA Sequencing. *Nucleic Acids Res.* **2023**, *51* (20), 11197−11212.
(44) Lucas, M. C.; Pryszcz, L. P.; Medina, R.; Milenkovic, I.; Camacho, N.; Marchand, V.; Motorin, Y.; Ribas De Pouplana, L.; Novoa, E. M. Quantitative Analysis of tRNA Abundance and Modifications by Nanopore RNA Sequencing. *Nat. Biotechnol.* **2024**, *42* (1), 72−86.
(45) Li, H.; Durbin, R. Fast and Accurate Short Read Alignment with Burrows−Wheeler Transform. *Bioinformatics* **2009**, *25* (14), 1754−1760.
(46) Workman, R. E.; Tang, A. D.; Tang, P. S.; Jain, M.; Tyson, J. R.; Razaghi, R.; Zuzarte, P. C.; Gilpatrick, T.; Payne, A.; Quick, J.; Sadowski, N.; Holmes, N.; De Jesus, J. G.; Jones, K. L.; Soulette, C. M.; Snutch, T. P.; Loman, N.; Paten, B.; Loose, M.; Simpson, J. T.; Olsen, H. E.; Brooks, A. N.; Akeson, M.; Timp, W. Nanopore Native RNA Sequencing of a Human Poly(A) Transcriptome. *Nat. Methods* **2019**, *16* (12), 1297−1305.
(47) Lai, H.; Feng, N.; Zhai, Q. Discovery of the Major 15−30 Nt Mammalian Small RNAs, Their Biogenesis and Function. *Nat. Commun.* **2023**, *14* (1), No. 5796.
(48) Shi, J.; Zhou, T.; Chen, Q. Exploring the Expanding Universe of Small RNAs. *Nat. Cell Biol.* **2022**, *24* (4), 415−423.
(49) Shi, J.; Zhang, Y.; Tan, D.; Zhang, X.; Yan, M.; Zhang, Y.; Franklin, R.; Shahbazi, M.; Mackinlay, K.; Liu, S.; Kuhle, B.; James, E. R.; Zhang, L.; Qu, Y.; Zhai, Q.; Zhao, W.; Zhao, L.; Zhou, C.; Gu, W.; Murn, J.; Guo, J.; Carrell, D. T.; Wang, Y.; Chen, X.; Cairns, B. R.; Yang, X.; Schimmel, P.; Zernicka-Goetz, M.; Cheloufi, S.; Zhang, Y.; Zhou, T.; Chen, Q. PANDORA-Seq Expands the Repertoire of Regulatory Small RNAs by Overcoming RNA Modifications. *Nat. Cell Biol.* **2021**, *23* (4), 424−436.
(50) Hendra, C.; Pratanwanich, P. N.; Wan, Y. K.; Goh, W. S. S.; Thiery, A.; Göke, J. Detection of m6A from Direct RNA Sequencing

Using a Multiple Instance Learning Framework. *Nat. Methods* **2022**, *19* (12), 1590−1598.
(51) Zhong, Z.-D.; Xie, Y.-Y.; Chen, H.-X.; Lan, Y.-L.; Liu, X.-H.; Ji, J.-Y.; Wu, F.; Jin, L.; Chen, J.; Mak, D. W.; Zhang, Z.; Luo, G.-Z. Systematic Comparison of Tools Used for m6A Mapping from Nanopore Direct RNA Sequencing. *Nat. Commun.* **2023**, *14* (1), No. 1906.
(52) Lange, T.; Stracke, S.; Rettig, R.; Lendeckel, U.; Kuhn, J.; Schlüter, R.; Rippe, V.; Endlich, K.; Endlich, N. Identification of miR-16 as an Endogenous Reference Gene for the Normalization of Urinary Exosomal miRNA Expression Data from CKD Patients. *PLoS One* **2017**, *12* (8), No. e0183435.



https://doi.org/10.1021/jacs.5c02808
*J. Am. Chem. Soc.* 2025, 147, 15614−15624